Int J Clin Exp Pathol 2018;11(9):4637-4643
www.ijcep.com /ISSN:1936-2625/IJCEP0083981

Original Article

Copy number variation in progression of inverted papilloma to squamous cell carcinoma of the nasal cavity

Dong Hoon Shin[1*], Jong-Kil Lee[2*], Kyu-Sup Cho[3], Hwan-Jung Roh[2]

Departments of [1]Pathology, [2]Otorhinolaryngology and Research Institute for Convergence of Biomedical Science and Technology, Pusan National University Yangsan Hospital, Yangsan, Republic of Korea; [3]Department of Otorhinolaryngology and Biomedical Research Institute, Pusan National University Hospital, Busan, Republic of Korea. [*]Equal contributors.

Received August 13, 2018; Accepted August 29, 2018; Epub September 1, 2018; Published September 15, 2018

Abstract: Inverted papilloma (IP) is a benign tumor occurring in nasal cavity. It can recur or progress to squamous cell carcinoma (SCC). The molecular mechanism of their biologic behavior is not fully revealed. Copy number variation (CNV) may contribute to progression of IP. We performed microarray comparative genome hybridization (aCGH). Five cases of IP, 2 cases of IP with dysplasia, 7 cases of SCC arising in a background of IP were submitted. The average numbers of somatic CNVs and copy number variable regions (CNVRs) were 991.9 and 866.9, respectively. Gain of 19p13.3, including 30 protein-coding genes, was observed in 2 IP and 7 SCC cases. Among those genes, BSG encoding the extracellular matrix metalloproteinase (MMP) inducer (EMMPRIN)/CD147 may play more important role in the progression of IP to SCC. Further study for validation of the aCGH result is necessary.

Keywords: Nasal cavity, inverted papilloma, squamous cell carcinoma

Introduction

An inverted papilloma (IP) is a sinonasal epithelium-derived tumor occurring in the nasal cavity and presenting as a polypoid mass [1]. It is a benign tumor but is clinically multifocal and locally aggressive. Although it is benign pathologically, it recurs after surgical resection and metachronous or synchronous squamous cell carcinoma (SCC) can develop [2]. The incidence of the malignant transformation of IP into SCC has been reported to be between 5 and 15% [2]. IP with synchronous carcinoma occurs when there is no history of a previously resected IP. Carcinoma may arise from the IP itself or may be observed as a separate lesion. IP with metachronous carcinoma develops at the site of a previously benign IP. According to a meta-analysis, rates of synchronous and metachronous carcinoma are 7.1% and 3.6%, respectively [2]. However, there are no documented histologic, radiographic, or pathologic findings predictive of malignant transformation to date.

Although the clinical and histological features of IP have been well described, the molecular basis of its pathogenesis, especially with regard to its progression to SCC, has yet to be elucidated. Thus, there are currently no known biomarkers for predicting progression and managing patient treatment according to stratified risks. In this study, we aimed to identify such biomarkers by performing a genome-wide screening of copy number abnormalities using microarray comparative genome hybridization (aCGH) of samples of IP, IP with dysplasia, and SCC arising from IP. We further investigated the probable relationships between genetic profiles and the clinical and pathologic characteristics of IP.

Materials and methods

Sample selection

Samples of IP, IP with dysplasia, and SCC arising from IP, archived at Pusan National University Hospital and Pusan National University Yang-San Hospital between 2005 and 2012, were searched. Among these, 5 cases of IP, 2 cases of IP with dysplasia, and 7 cases of SCC arising from IP were selected based on preser-

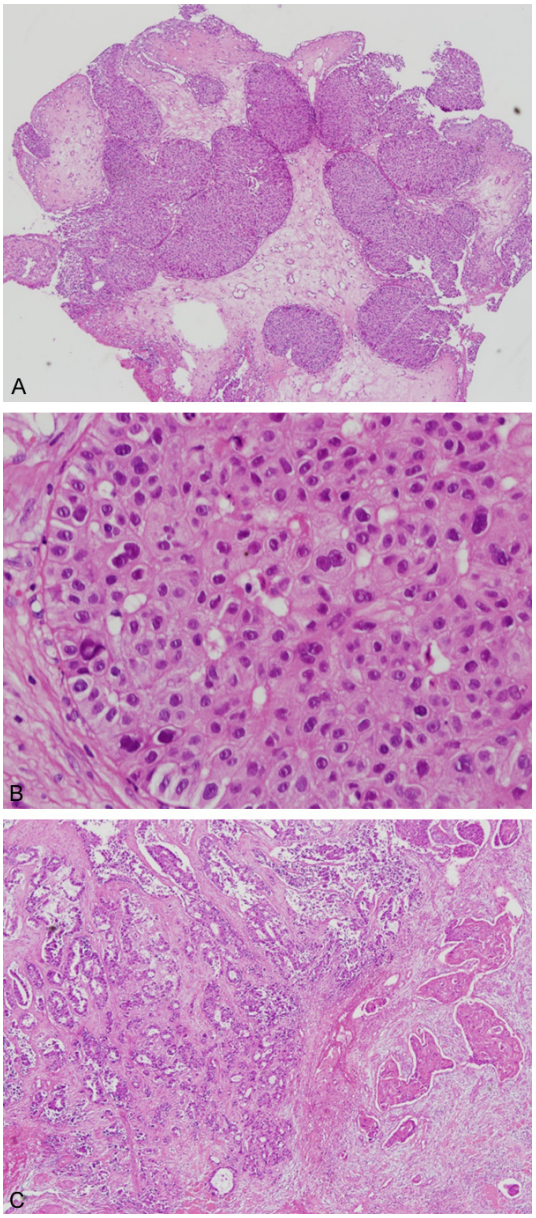

Figure 1. Microscopic features of inverted papilloma (A), dysplastic change in inverted papilloma (B), and squamous cell carcinoma arising from inverted papilloma (C).

vation status and the specimen sizes of formalin-fixed paraffin-embedded (FFPE) tissue blocks. A matched pair of IP and IP with dysplasia was available from a single patient. Another matched pair of IP and SCC arising from IP was derived from a different individual patient.

Microarray experiment

To screen for somatic DNA copy number variations (SCNVs), we used the MAC Array Karyo 4000 (Macrogen Inc., Seoul, Korea) spotted with 4,030 human (BAC) clones and covering the entire human genome at a resolution of 1 Mb. Array-based CGH was performed as previously reported. After tumor DNA (500 ng) was extracted from FFPE tissues, normal male DNA and digested tumor DNA were labeled with Cy5-dCTP and Cy3-dCTP, respectively, by random primer labeling (Array CGH Genomic Labeling System; Invitrogen, Carlsbad, CA, USA). Then, the labeled DNA was washed, its yield was quantified, and the appropriate control and test samples were combined in equal amounts. Hybridizations were performed in a sealed chamber for 48 h at 37°C. After hybridization, slides were scanned on a GenePix 4200A two-color fluorescent scanner (Axon Instruments, Union City, CA, USA). The captured images were analyzed using GenePix Pro 4.1 imaging software (Axon Instruments). Average $\log_2$ Cy3/Cy5 signal ratios of triplicate BAC clones were calculated for each sample, and ± 0.25 $\log_2$ ratio was used as a threshold for defining copy number gains and losses.

Real-time PCR

PCR reactions were performed on an ABI Prism 7700 Sequence Detection System and an ABI Prism5700 SDS (Applied Biosystems, Carlsbad, CA, USA), which yielded similar results (data not shown). Amplification mixtures for determination of the copy numbers of *CA9, BSG,* and *PRSS57* consisted of template DNA, 500 nM of each primer, 200 nM of TaqMan probe, and TaqMan Universal PCR Master Mix (Applied Biosystems). The cycling conditions were as follows: 10 minutes of polymerase activation at 95°C, followed by 40 cycles at 95°C for 15 seconds and 60°C for 1 minute. Relative quantification of target genes was performed by comparison with the reference, RNase P, for which copy number is similar among all normal human and neoplastic cells. Copy number changes (relative to RNase P) in target genes in tumors compared with those in paired normal tissues were determined using the formula: $(\text{Target/RNase P})_{\text{tumor}}/(\text{Target/RNase P})_{\text{paired normal}}$.

Results

Clinicopathologic findings

For aCGH analyses, 9 patients were enrolled. Four patients had IP and four other patients

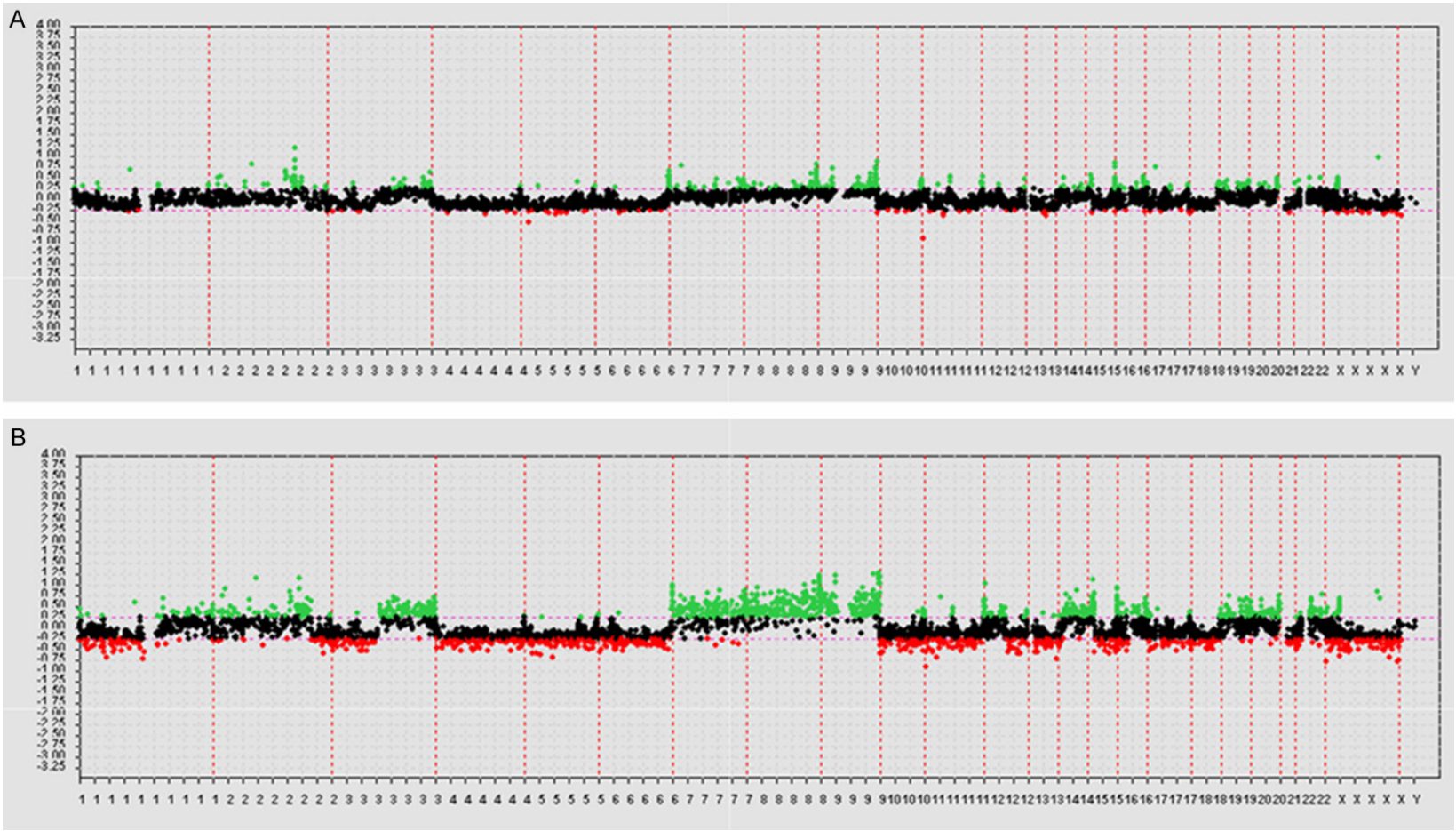

Figure 2. Representative scatter plot of inverted papilloma (A) and squamous cell carcinoma arising from inverted papilloma (B). Green and red dots indicate gains and losses respectively.

Table 1. Numbers of somatic copy number variations (SCNVs) and copy number variable regions (CNVRs)

Sample	SCNVs	CNVRs
IP	783	681
IP with dysplasia	1500	1325
SCC	996	869

IP, inverted papilloma; SCC, squamous cell carcinoma.

had SCC, while one patient provided both IP and SCC samples. Five of the patients experienced IP recurrence. One patient expired due to SCC. Pathologic features of inverted IP, IP with dysplasia, and SCC is presented in **Figure 1**.

Individual assays to determine the copy numbers of *CA9, BSG,* and *PRSS57* were performed with samples from 8 patients, including 3 SCC and 6 IP cases. Male were 15 and female were 5. Mean age at the time of diagnosis was 60.4. Three patients with IP experienced recurrence.

aCGH analyses

Copy number profiles were obtained from 14 samples (**Figure 2**). The average numbers of SCNVs and copy number variable regions (CNVRs) were 991.9 and 866.9, respectively. There were an average of 615.9 and 375.9 gains and losses, respectively, among the samples. When grouped by IP, dysplasia, and SCC, mean values of CNVRs were 681.4, 1324.5, and 868.6 (**Table 1**). Most SCNV sizes fell in the range of 10-500 kb, with none over 500 kb. Among 856 cytoband regions affected, the most dramatic change was detected in 16p13.3, with 252. There were 19 regions that harbored more than 100 changes each. Five regions were found to be significantly associated with IP, dysplasia, and SCC. By omitting the dysplasia group, 2 additional regions were identified (**Table 2**). There were 34 gains and 11 losses. In particular, a gain in 19p13.3 was observed in 2 IP samples and 7 SCC samples. There were 40 protein-coding genes detected in CNVRs. Among these, 8 were found to be related to various cancers according to a thorough literature search.

Copy number assay for CA9, PRSS57, and BSG

Mean copy numbers for *CA9*, *PRSS57*, and *BSG* were 2.25, 2.92, and 2.90, respectively (**Table 3**). When copy numbers for IP and SCC were considered separately, the mean values for *CA9*, *PRSS57*, and *BSG* were 2.37, 3.30, and 3.11 respectively for IP and 2.01, 2.18, and 2.47 respectively for SCC.

Discussion

While IPs are benign tumors, when not completely resected, they can recur and rarely progress to SCC with a risk of SCC of about 10% [1, 2]. A better understanding of the biology of IP may aid in treating IP and preventing its progression to SCC, as the detailed molecular mechanisms of its pathogenesis, progression, or recurrence are not currently fully understood. While several studies have been conducted to reveal the molecular basis of IP pathogenesis, research focusing on SCNVs is scarce [3]. To our knowledge, this is the first genome-wide copy number analysis of IP and SCC arising from IP. An oligonucleotide-based aCGH technique was used to identify small gains or losses in FFPE archived tissues. Generally, genes associated with copy number gains are likely to be oncogenes when involved in the pathogenesis of cancer [4]. In contrast, genes associated with copy number losses are usually tumor suppressor genes [4]. In this study, 18 CNVRs were detected among all 14 samples, and all of these represented copy number gains. The genes involved in these CNVRs may be involved in the early pathogenesis of IP, as they were detected in both IP and SCC cases. Copy number losses were observed less frequently in this study, suggesting that oncogenes are more actively involved in the pathogenesis of IP than tumor suppressors.

Among 330 CNVRs that were observed in over 7 out of the 14 samples, 265 CNVRs exhibited only gains in the affected samples, while 32 CNVRs revealed only losses. If SCNVs are drivers of abnormalities, they may be consistently associated with only gains or losses and more frequently detected in SCC than IP cases. In this regard, several CNVRs were presumed to be associated with the progression of IP. A loss at 3p14.2, containing the *FHIT* gene, was detected in 2 IP, 2 IP with dysplasia, and 5 SCC cases. *FHIT* is a tumor suppressor that is frequently deleted in carcinomas of the lung, head and neck, stomach, cervix, breast, and kidney. The $\log_2$ ratio of *FHIT* was greater than -1.0, indicating a heterozygous loss. The loss of *FHIT*

Table 2. Statistically significant copy number variable regions and genes

CNVR	Size	CB	Loss	Gain	IP	Dys	SCC	Genes	*P* value
chr2:109953762-110091100	137338	q13	2	4	0	1	5	LIMS3, RGPD5, RGPD6	0.03
chr9:35618094-35811244	193150	p13.3	0	6	4	2	0	CA9, CCDC107, CD72, CREB3, GBA2, HINT2, LZIP, NPR2, PC3, RGP1, SIT1, SPAG8, TLN1, TPM2	0.002
chr11:51526726-51583396	56670	p11.11	4	1	3	2	0	OR4C46	0.01
chr11:108050610-108170706	120096	q22.3	3	0	3	0	0	DDX10	0.06
chr14:106796264-106988959	192695	q32.33-NA	2	2	3	1	0	IGHV7-81	0.03
chr17:456304-598092	141788	p13.3	0	3	3	0	0	FAM57A, GEMIN4, VPS53	0.06
chr19:502845-658531	155686	p13.3	0	9	2	0	7	BSG, FGF22, FSTL3, HCN2, POLRMT, PRSSL1, RNF126	0.01
chr19:13008000-13263279	255279	p13.13	0	9	5	2	2	CACNA1A, IER2, LYL1, NACC1, NFIX, STX10, TRMT1	0.02

Table 3. Results of TaqMan copy number assays for individual genes

Gene	Mean copy number	*P* value
CA9	2.54	0.20
BSG	2.90	0.12
PRSS57	2.92	0.15

may be important in the progression of IP to SCC.

Loss at 2q13 was observed in 1 dysplasia and 4 SCC cases but not in IP. This region contained 8 protein-coding genes, including *EFA6B, LIMS3, NPHP1, PAX8, RANBP2, RGPD5, RGPD6,* and *SLC5A7*. *PAX8* and *RANBP2* are expressed in thyroid follicular carcinoma [5] and inflammatory myofibroblastic tumors [6], respectively. Because these genes are oncogenes, loss is less likely to play an important role.

Moreover, gain of 19p13.3, including 30 protein-coding genes, was observed in 2 IP and 7 SCC cases. Among these genes, *BSG* encodes the extracellular matrix metalloproteinase (MMP) inducer (EMMPRIN)/CD147, which is highly expressed on the tumor cell surface [7]. This transmembrane molecule induces the expression of MMPs in fibroblasts and tumor cells and is related to the progression of many cancers [7-11]. In head and neck SCC, it has been suggested that it promotes protease activity to increase invasiveness and metastasis [8-10]. Notably, this region contains 7 genes related to inflammatory cell function. This includes *PRTN3, GZMM, PRSS57*, and *ELA2,* which encode proteases secreted by inflammatory cells [11]. It also includes *AZU1*, which encodes a chemotactic glycoprotein stored in neutrophils, and complement factor D (*CFD*) [11]. Recently, tumor-associated neutrophils have been regarded as one of the key components in carcinogenesis [12]. The elastase secreted by neutrophils can provoke tissue damage, creating a favorable tissue environment for tumorigenesis and its progression. The production of these proteases by the tumor itself may also play an oncogenic role, similar to that of neutrophil-secreted factors. One study showed that BSG expression in nasopharyngeal carcinoma is accompanied by the overexpression of GZMM, FGF22, AZU1, FSTL3, PRTN3, and PRSS57, which are all located at 19p13.3 [13]. This result is consistent with that of the present study. BSG has been reported to recruit neutrophils, and therefore, tumor-based BSG expression can further promote tumor progression by recruiting tumor-associated neutrophils.

Gain at 9p13.3 was observed in 4 IP and 2 IP with dysplasia cases but not in SCC cases. The underlying reason for this difference is not clear. In order to further investigate this difference, three genes in this region were selected for further examination. This included BSG and PRSS57, as well as carbonic anhydrase 9 (CA9), an important downstream molecule of hypoxia-inducible factor-1 alpha (HIF-1α) that is known to be associated with tumor progression in various cancers under hypoxic environments [14]. TaqMan probes were used to perform copy number assays in 6 IP and 3 SCC cases, including 2 matched pairs of IP and SCC samples from the same individual. In one pair, the copy number of *CA9* was 1.8 and 3.0 in IP and SCC, respectively. In the other pair, the values were 2.3 and 1.9, respectively. The average

copy number in the other SCC cases was 1.2. Thus, it seems that changes in the copy of *CA9* are variable across samples and that a gain in copy number at 9p13.3 may be a passenger SCNV. This result should be investigated further using additional samples. In the cases of *BSG* and *PRSS57*, the mean copy numbers in IP cases were 3.3 and 3.1, respectively, while those in SCC were 2.2 and 2.5, respectively. Simultaneous gains in *BSG* and *PRSS57* are consistent with the aCGH results and suggest that 19p13.3 gain is a driver of SCNV.

Copy number alterations in head and neck SCC have been well studied [15]. The most frequent changes are gains at 3q26, 8q24, and 11q13, which include phosphatidylinositol 3-kinase (*PI3K*), catalytic alpha subunit (*PIK3CA*), c-Myc (*MYCC*), and cyclin D1 (*CCND1*). Changes in 3q-26 and 11q13 were observed in 4 and 3 samples, respectively, in this study. Our data also showed 8q24 amplification in 13 samples, excluding 1 IP with dysplasia, but the CNVR did not contain MYCC. Hence, it can be assumed that the molecular processes by which SCC arises from IP may involve a unique pathway that differs from other head and neck SCCs.

Limitations of this study include the small number of samples included, in particular the limited number of paired normal-IP-dysplasia-SCC samples. Because most IP and SCC samples are obtained via biopsy, it is difficult to access a large number of samples, which is a critical issue for molecular studies. Therefore, investigations into genetic changes are often discouraged. For further studies, prudent design and sample preparation are required.

Moreover, to confirm the role of BSG and proteases (including PRSS57) in IP progression, their expression at the protein level should be examined to determine whether tumor cells produce these proteins. Upon establishing the role of BSG and PRSS57, anti-protease therapy may represent a new method for preventing the progression of IP to SCC.

In conclusion, this study involved a genome-wide copy number analysis of IP, IP with dysplasia, and SCC and identified BSG and PRSS57 as candidate oncogenes.

Disclosure of conflict of interest

None.

Address correspondence to: Dr. Hwan-Jung Roh, Department of Otorhinolaryngology, Pusan National University Yangsan Hospital, Beom-eo li, Mul-geum eup, Yang-san si, Gyeongsangnam-do 626-770, Republic of Korea. E-mail: rohhj@pusan.ac.kr

References

[1] Sauter A, Matharu R, Hörmann K, Naim R. Current advances in the basic research and clinical management of sinonasal inverted papilloma (review). Oncol Rep 2007; 17: 495-504.

[2] Mirza S, Bradley PJ, Acharya A, Stacey M, Jones NS. Sinonasal inverted papillomas: recurrence, and synchronous and metachronous malignancy. J Laryngol Otol 2007; 121: 857-864.

[3] Stephen JK, Vaught LE, Chen KM, Sethi S, Shah V, Benninger MS, Gardner GM, Schweitzer VG, Khan M, Worsham MJ. Epigenetic events underlie the pathogenesis of sinonasal papillomas. Mod Pathol 2007; 20: 1019-1027.

[4] Michels E, De Preter K, Van Roy N, Speleman F. Detection of DNA copy number alterations in cancer by array comparative genomic hybridization. Genet Med 2007; 9: 574-584.

[5] Batista FA, Ward LS, Marcello MA, Martins MB, Peres KC, Torricelli C, Bufalo NE, Soares FA, da Silva MJ, Assumpção LV. Gene expression of thyroid-specific transcription factors may help diagnose thyroid lesions but are not determinants of tumor progression. J Endocrinol Invest 2016; 39: 423-429.

[6] Patel AS, Murphy KM, Hawkins AL, Cohen JS, Long PP, Perlman EJ, Griffin CA. RANBP2 and CLTC are involved in ALK rearrangements in inflammatory myofibroblastic tumors. Cancer Genet Cytogenet 2007; 176: 107-114.

[7] Zheng HC, Takahashi H, Murai Y, Cui ZG, Nomoto K, Miwa S, Tsuneyama K, Takano Y. Upregulated EMMPRIN/CD147 might contribute to growth and angiogenesis of gastric carcinoma: a good marker for local invasion and prognosis. Br J Cancer 2006; 95: 1371-1378.

[8] Suzuki S, Ishikawa K. Combined inhibition of EMMPRIN and epidermal growth factor receptor prevents the growth and migration of head and neck squamous cell carcinoma cells. Int J Oncol 2014; 44: 912-917.

[9] Huang Z, Tan N, Guo W, Wang L, Li H, Zhang T, Liu X, Xu Q, Li J, Guo Z. Overexpression of EMMPRIN isoform 2 is associated with head and neck cancer metastasis. PLoS One 2014; 9: e91596.

[10] Sweeny L, Liu Z, Bush BD, Hartman Y, Zhou T, Rosenthal EL. CD147 and AGR2 expression promote cellular proliferation and metastasis of head and neck squamous cell carcinoma. Exp Cell Res 2012; 318: 1788-1798.

[11] Caughey GH. A pulmonary perspective on GASPIDs: granule-associated serine peptidases of immune defense. Curr Respir Med Rev 2006; 2: 263-277.
[12] Sun Z, Yang P. Role of imbalance between neutrophil elastase and alpha 1-antitrypsin in cancer development and progression. Lancet Oncol 2004; 5: 182-190.
[13] Gao L, Zhong JC, Huang WT, Dang YW, Kang M, Chen G. Integrative analysis of BSG expression in NPC through immunohistochemistry and public high-throughput gene expression data. Am J Transl Res 2017; 9: 4574-4592.
[14] Harris AL. Hypoxia–a key regulatory factor in tumour growth. Nat Rev Cancer 2002; 2: 38-47.
[15] Gollin SM. Chromosomal alterations in squamous cell carcinomas of the head and neck: window to the biology of disease. Head Neck 2001; 23: 238-253.